Langmuir, **23** (10), 5338 -5351, 2007. 10.1021/la062612o S0743-7463(06)02612-6
Web Release Date: April 12, 2007

Characterization of Fractal Particles Using Acoustics, Electroacoustics, Light Scattering, Image Analysis, and Conductivity

A. S. Dukhin,† D. Fluck,† P. J. Goetz,† V. N. Shilov,‡ and S. S. Dukhin*†

Dispersion Technology Inc., Bedford Hills, New York 10507, and Institute of Bio-Colloid Chemistry, Kiev, Ukraine

Received September 6, 2006

In Final Form: January 22, 2007

Abstract:

Fractals are aggregates of primary particles organized with a certain symmetry defined essentially by one parameter-a fractal dimension. We have developed a model for the interpretation of acoustic data with respect to particle structure in aggregated fractal particles. We apply this model to the characterization of various properties of a fumed silica, being but one example of a fractal structure. Importantly, our model assumes that there is no liquid flow within the aggregates (no advection). For fractal dimensions of less than 2.5, we find that the size and density of aggregates, computed from the measured acoustic attenuation spectra, are quite independent of the assumed fractal dimension. This aggregate size agrees well with light-scattering measurements. We applied this model to the interpretation of electroacoustic data as well. A combination of electroacoustic and conductivity measurements yields sufficient data for comparing the fractal model of the particle organization with a simple model of the separate primary particles. Conductivity measurements provide information on particle surface conductivity reflected in terms of the Dukhin number (*Du*). Supporting information for the ζ potential and *Du* can also be provided by electroacoustic measurements assuming thin double-layer theory. In comparing values of *Du* from these two measurements, we find that the model of separate solid particles provides much more consistent results than a fractal model with zero advection. To explain this, we first need to explain an apparent contradiction in the acoustic and electroacoustic data for porous particles. Although not important for interpreting acoustic data, advection within the aggregate does turn out to be essential for interpreting electrokinetic and electroacoustic phenomena in dispersions of porous particles.

BATCH: la5b59 USER: amh29 DIV: @xyv04/data1/CLS_pj/GRP_la/JOB_j11/DIV_la062612o DATE: April 4, 2007

Characterization of Fractal Particles Using Acoustics, Electroacoustics, Light Scattering, Image Analysis, and Conductivity

A. S. Dukhin,[†] D. Fluck,[†] P. J. Goetz,[†] V. N. Shilov,[‡] and S. S. Dukhin*,[†]

Dispersion Technology Inc., Bedford Hills, New York 10507, and Institute of Bio-Colloid Chemistry, Kiev, Ukraine

Received September 6, 2006. In Final Form: January 22, 2007

Fractals are aggregates of primary particles organized with a certain symmetry defined essentially by one parameter—a fractal dimension. We have developed a model for the interpretation of acoustic data with respect to particle structure in aggregated fractal particles. We apply this model to the characterization of various properties of a fumed silica, being but one example of a fractal structure. Importantly, our model assumes that there is no liquid flow within the aggregates (no advection). For fractal dimensions of less than 2.5, we find that the size and density of aggregates, computed from the measured acoustic attenuation spectra, are quite independent of the assumed fractal dimension. This aggregate size agrees well with light-scattering measurements. We applied this model to the interpretation of electroacoustic data as well. A combination of electroacoustic and conductivity measurements yields sufficient data for comparing the fractal model of the particle organization with a simple model of the separate primary particles. Conductivity measurements provide information on particle surface conductivity reflected in terms of the Dukhin number (Du). Supporting information for the ζ potential and Du can also be provided by electroacoustic measurements assuming thin double-layer theory. In comparing values of Du from these two measurements, we find that the model of separate solid particles provides much more consistent results than a fractal model with zero advection. To explain this, we first need to explain an apparent contradiction in the acoustic and electroacoustic data for porous particles. Although not important for interpreting acoustic data, advection within the aggregate does turn out to be essential for interpreting electrokinetic and electroacoustic phenomena in dispersions of porous particles.

Introduction

Fractals are aggregates of primary dispersed particles with a certain structural symmetry that reproduces itself from one spatial level to another. The notion of fractals was introduced almost 30 years ago by Mandelbrot[1-3] and is a widely accepted model for describing coagulation phenomena.

Fractal aggregates contain a certain amount of trapped liquid inside, which makes their characterization much more challenging comparing to that of usual solid nonporous particles. We use a combination of several techniques to characterize these complex particles. It turns out that different techniques require different models of particles, especially with regard to advection, which is liquid flow through the particle interior. In some cases, we can simply ignore advection, but in other cases, advection is essential for a proper description of the observed phenomenon.

The amount of trapped liquid can be quantified by one of three different parameters. The first way to describe this trapped liquid is by a porosity χ that represents the volume ratio of the liquid and solid phases inside the aggregate. An alternative parameter that can be used to describe the trapped liquid is the density of the aggregate ρ_{agg}, which is different than the density of the primary particles ρ_p or the density of the liquid media ρ_m. Finally, we should distinguish between the volume fraction of the dispersed phase φ_{agg} in the dispersion and the volume fraction of solids φ_{solids}.

Of all these parameters, only φ_{solids} is easily measurable with a pycnometer. Neither the aggregate volume fraction φ_{agg} nor the volume fraction of solids inside the aggregate φ_{in} is measurable with a pycnometer. The aggregate density ρ_{agg} is also not easily measurable.

However, there are known means for measuring the aggregates size. Light scattering offers one opportunity, as described in refs 4 and 5. Acoustic attenuation spectroscopy is also suitable for this purpose, as will be discussed in detail in this article.

We will show that acoustics yields information on aggregate size practically independently on the fractal number and ignoring advection. We do this experimentally using chemical mechanical polishing (CMP) silica slurry SS-25 produced by Cabot Corporation.

There is a large body of theoretical and experimental work dedicated to the hydrodynamic and mechanical properties of fractals, but very little is known about their electrical and especially their electrokinetic properties.

However, several electrokinetics papers are dedicated not specifically to fractals but to porous particles.[6-11] These papers can then serve as a basis for interpreting the electrokinetics of fractals. They describe several peculiarities of porous particles that are important for fractals as well.

The first one is associated with the additional electric conductivity inside a fractal aggregate. The fractal interior contains

* Dispersion Technology Inc.
‡ Institute of Bio-Colloid Chemistry.

(1) Mandelbrot, B. B. *The Fractal Geometry of Nature*; W. H. Freeman: New York, 1982.
(2) Meakin, P. *Adv. Colloid Interface Sci.* **1988**, *28*, 249−331.
(3) Meakin, P.; Vicsek, T.; Family, F. *Phys. Rev. B* **1985**, *31*, 564.
(4) Hua, W.; Lattuada, M.; Sandkuhler, P.; Sefcik, J.; Morbidelli, M. *Langmuir* **2003**, *19*, 10711−10718.
(5) Sandkuhler, P.; Lattuada, M.; Hua, W.; Sefcik, J.; Morbidelli, M. *Adv. Colloid Interface Sci.* **2005**, *113*, 65−83.
(6) Simonov, I. N.; Shilov, V. N.; Petkanchin, I. B.; Sidorova, M. P. *Dopov. Ukr. SSR B* **1974**, *6*, 556.
(7) Ohshima, H. *Adv. Colloid Interface Sci.* **1995**, *62*, 89.
(8) Ohshima, H. *Colloids Surf., A* **1995**, *103*, 249.
(9) Miller, N. P.; Berg, J. C.; O'Brien, R.W. *J. Colloid Interface Sci.* **1992**, *153*, 236−243.
(10) Miller, N. P.; Berg, J. C. *J. Colloid Interface Sci.* **1993**, *159*, 253.
(11) Velegol, D.; Andreson, J.; Solomentsev, Y. In *Interfacial Electrokinetics and Electrophoresis*; Delgado, A.V., Ed.; Marcel Decker: New York, 2002; Chapter 6.

10.1021/la062612o CCC: $37.00
Published on Web 00/00/0000 PAGE EST: 13.4

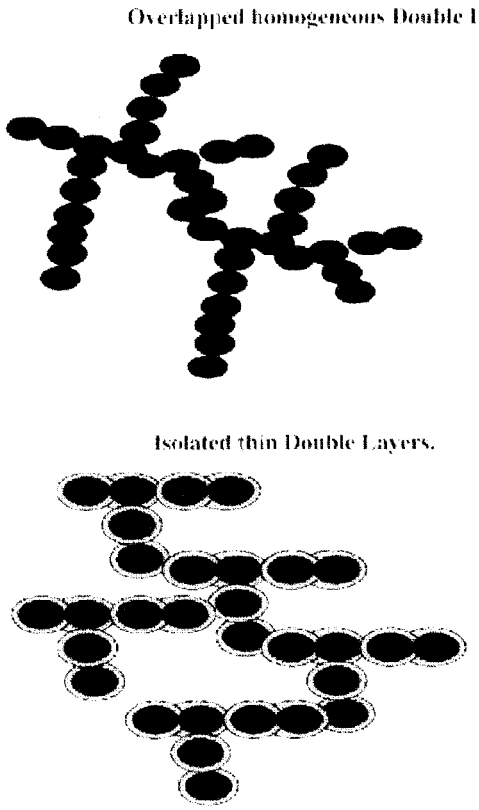

Figure 1. Two extreme cases of the double-layer structure inside the pores.

double layers surrounding the primary particles. The electrolyte solution within the double layer is more conducting than the exterior medium. It is important to take into account that this excessive internal conductivity is associated with counter ions only, either anions or cations depending on the sign of the surface charge. The ions transfer numbers inside the fractal may be quite different as compared to that in the bulk as a result of the different concentration of ions there. Any difference would result in a concentration polarization of the fractal.

The next peculiar feature of fractals is that the external electric field generates electrosmotic flow inside the aggregate. The electric field penetrates inside and moves electric charges of the diffuse layer surrounding the primary particles inside the aggregate. The ion motion involves the surrounding liquid, which generates macroscopic flow known as electrosmosis.

All of these effects depend on the structure of the double layer inside the fractal aggregate. This structure is quite complex because of the intricate network of channels inside the aggregate. We do not know how to describe it in general, for any foreseeable channel structure. Fortunately, there are two simple cases for which the channel structure is not important. They are described in some detail in the Theory section.

The first case corresponds to the well-known approximation of a thin DL in which we assume that the ratio of the Debye length κ^{-1} to the radius of primary particles a_1 is very small. This assumption is valid for sufficiently high ionic strength for a given primary particle radius.

When the DLs are much thinner that the average thickness of the channels, they do not overlap. For this first case of both thin and non-overlapped DL's, the theory becomes tremendously simplified. It is usually referred to as the thin isolated DL model. The electrophoretic mobility of porous or fractal particles with thin DL is simply identical to the Smoluchowski mobility of the primary particle if the surface conductivity is negligible. This follows directly from a wonderful feature of Smoluchowski's theory in which the electrophoretic mobility is independent of the shape of the moving object.[12,13] This fact is well known in the literature. For instance, a short study by Anderson and Velegol[11] leads to the same conclusion.

This equality of the aggregate and primary particle electrophoreric mobility presents one interesting paradox for electroacoustic measurements.

There are two version of electroacoustics depending on the driving force. In the case of ultrasound as the driving force, the electric signal is a measured output. It is called colloid vibration current (CVI). In the opposite case when the electric field is a driving force, the ultrasound signal is the measured output. It is called the electricsonic amplitude (ESA).

According to the Onsager principle,[14] these two effects should be symmetrical.

In the case of the porous aggregate, this symmetry becomes questionable because the electric and hydrodynamic fields are not symmetrical with regard to penetrating the inside the aggregate. The electric field does penetrate inside even at very low porosity. On the other side, an aggregate with low porosity is not penetrable with respect to hydrodynamic flow. It looks like this obvious comparison creates asymmetry under the driving force of electroacoustics. This would lead to the problem in understanding the Onsager principle validity for the aggregates.

The analysis and proof that the Onsager principle holds for the electroacoustics of the aggregates is given in the Appendix. This theoretical analysis concludes that advection is an essential feature of porous aggregate electrokinetics and must always be taken into account.

To verify theoretical predictions for porous fractal particles, we apply a combination of acoustic, electroacoustic, conductivity, and light-scattering measurements of the same fumed silica slurry. This is known in the literature as an example of fractal system.[3-5,9,10]

We use three different models to interprete these experimental data.

A separate particles model presents a dispersed phase consisting of separate primary particles with a size given by image analysis.

A porous particles model presents a dispersed phase consisting of porous particles with no advection and no particular internal structure.

A fractal particles model combines primary particles in fractal aggregates. It differs from the porous particle model by the fractal relationship among aggregate size, primary size, and particle porosity χ, as described below.

Only a model of separate particles takes into account advection, whereas two other models completely neglect it by considering particles to be impenetrable to liquids.

It turns out that the fractal particle model yields consistent results on the particle size for acoustics and light scattering. This means that advection is not important for these phenomena.

On the other hand, the fractal particle model fails for conductivity and electroacoustic measurements. These techniques

(12) Smoluchowski, M. In *Handbuch der Electrizitat und des Magnetismus*; Vol. 2, Barth: Leipzig, Germany, 1921.

(13) Dukhin, S. S.; Derjaguin, B. V. Electrokinetic Phenomena. In *Surface and Colloid Science*; Matijevic, E., Ed.; John Wiley & Sons: New York; Vol. 7, 1974.

(14) Onsager, L. *Phys. Rev.* **1931**, *37*, 405. Onsager, L. *Phys. Rev.* **1931**, *38*, 2265.

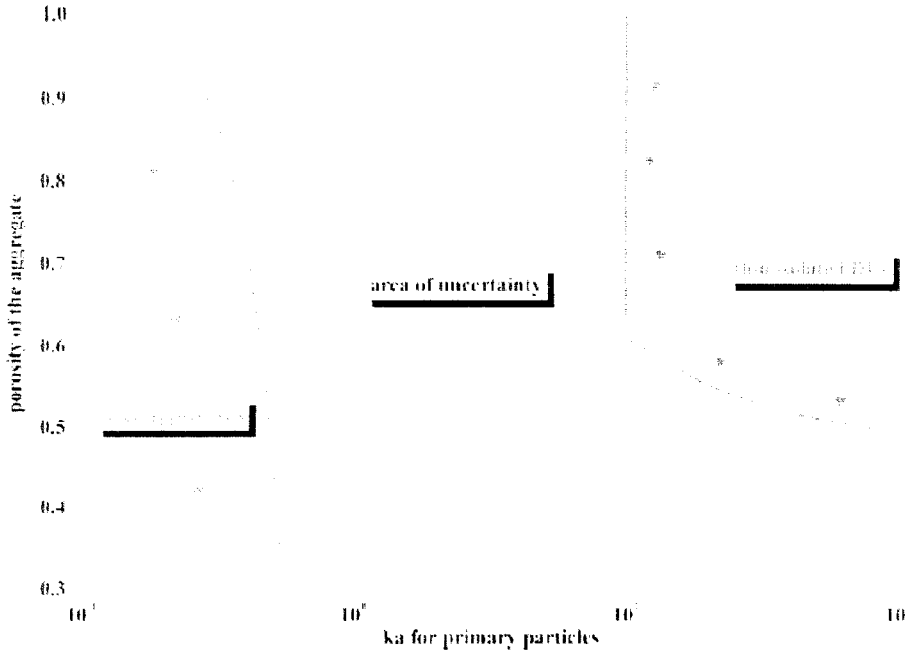

Figure 2. Approximate diagram that illustrates the dependence of the internal DL structure on the aggregate porosity and ka of the primary particles.

can be reconciled with the separate particles model, as expected on the basis of theoretical analysis.

Theory

We present here a description of the three different particles models that are applied later for interpreting experimental data. We also present here elements of theory that are relevant for interpreting experimental data. Acoustic theory and conductivity theory do not contain any novel results, whereas electroacoustic theory does. It is related to the validity of the Onsager principle for the porous particles. We present these new results derived by Shilov in the Appendix.

Models of Particles. We discuss here three different models of particles that allow us to link particle properties with properties of the solid material. Figure 3 illustrates these models.

Model of Separate Homogeneous Solid Particles Referred to Below as the Separate Particles Model. This is the usual model for characterizing dispersions and emulsions. We simply assume that particles consist only of the dispersed phase material. This yields a simple relationship between densities and weight fractions

$$\rho_p = \rho_s \tag{1}$$

$$w_p = w_s \tag{2}$$

where index p corresponds to the dispersed phase and index s corresponds to the solid material.

Model of Porous Particles Referred to Below as the Porous Particles Model. This model takes into account the possibility that part of the liquid would be trapped inside the particles with a complex shape. This might occur either for naturally porous materials or for aggregated particles that are built up from primary solid particles. This model introduces an additional parameter for characterizing particles, porosity χ. It is a volume fraction of the dispersion medium trapped inside the particle. This model yields the following equations for the relationship between density and weight fraction:

$$\rho_p = (1 - \chi)(\rho_s - \rho_m) + \rho_m \tag{3}$$

$$\varphi_p = \frac{\varphi_s}{1 - \chi} = \frac{w_s \rho_m}{(1 - \chi)[w_s \rho_m + (1 - w_s)\rho_s]} \tag{4}$$

The nature of this model eliminates the possibility of advection.

$$w_p = w_s \left[1 + \frac{\chi \rho_m}{(1 - \chi)\rho_s}\right] \tag{5}$$

which is liquid motion through the particle, because we consider the liquid inside the pores to be trapped and moving together with the particle.

Model of Fractal Particles Referred to Below as the Fractal Model. There is a simple relationship between the radius of a fractal aggregate that contains i particles (a_i) and the radius of primary particles a_1 given by

$$\frac{a_i}{a_1} = k_f i^{1/d_f} \tag{6}$$

The two parameters in this equation describe various types of aggregate structures. The k_f parameter is less important, and its value is typically very close to 1; therefore, we omit our consideration of it further analysis. The d_f parameter is more important and usually goes by the name of fractal dimension. For typical dispersions, this number varies roughly from 1 to 3. It equals 3 for coalescing emulsion droplets. The range of 2.1–2.2 corresponds to reaction-limited coagulation that results in rather compact aggregates. Smaller values of this fractal dimension of less than 1.8 are typical for diffusion-limited

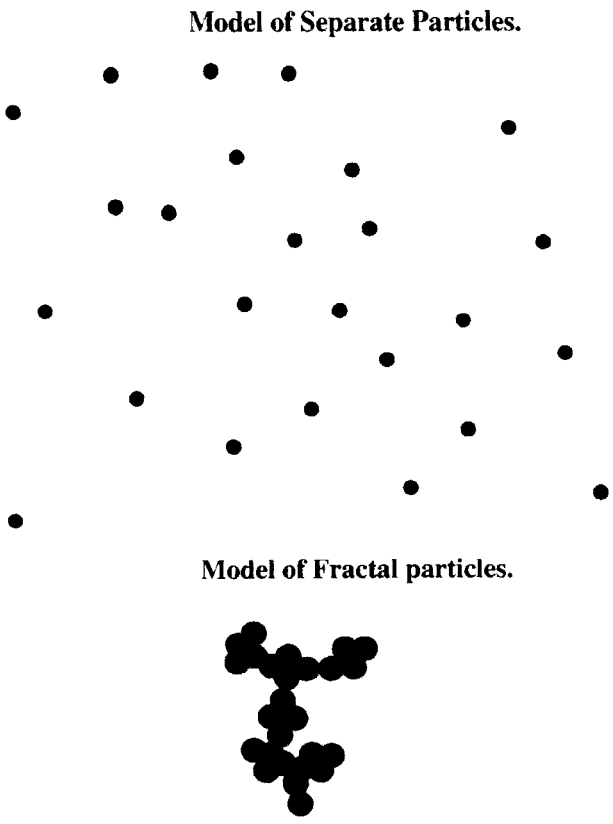

Figure 3. Two models applied for characterizing the dispersed phase in this article.

coagulation with loose flocs. Finally, a fractal dimension equal to 1 represents linear chain aggregates.[15-19]

Fractal aggregates contain a certain amount of trapped liquid inside. The amount of such trapped liquid can be quantified by one of three different parameters. The first way to describe this trapped liquid is by porosity χ that represents the volume ratio of the liquid and solid phases inside the aggregate

$$\chi = 1 - \varphi_{in} = 1 - \left(\frac{a_i}{a_1}\right)^{-3+d_f} \tag{7}$$

where φ_{in} is the volume fraction of the solid phase inside the aggregate.

An alternative parameter that can be used to describe the trapped liquid is the density of the aggregate ρ_{agg} which is different from the density of the primary particles ρ_p or the density of the liquid media ρ_m and is given by

$$\rho_{agg} = \left(\frac{a_i}{a_1}\right)^{3+d_f} (\rho_p - \rho_m) + \rho_m \tag{8}$$

A larger volume of aggregates leads to a larger volume fraction of the dispersed phase φ_{agg} in the dispersion compared to the volume fraction of solids φ_{solids}:

$$\frac{\varphi_{agg}}{\varphi_{solids}} = \left(\frac{a_i}{a_1}\right)^{3-d_f} \tag{9}$$

Of the three defined volume fractions, only φ_{solids} is easily measurable with a pycnometer. Neither the aggregate volume fraction φ_{agg} nor the volume fraction of solids inside the aggregate φ_{in} is measurable with a pycnometer. The aggregate density ρ_{agg} is also not easily measurable.

This model also ignores advection.

Double-Layer Models. The structure of the double layer inside the aggregates is quite complex because of the intricate network of the inside channels. We do not know how to describe it in general for any foreseeable channel structure. Fortunately, there are two simple cases for which the channel structure is not important.

The first case corresponds to the well-known approximation of a thin DL in which we assume that the ratio of the Debye length κ^{-1} to the radius of primary particles a_1 is very small:

$$\kappa a_1 \gg 1 \tag{10}$$

This assumption is valid for sufficiently high ionic strength for a given primary particle radius.

When the DLs are much thinner than the average thickness of the channels, they do not overlap. For this first case of both thin and nonoverlapped DL's, the theory becomes tremendously simplified. It is usually referred to as the thin isolated DL model.

In contrast, the second simplified case corresponds to completely overlapped DLs. The more the DLs are overlapped, the less important their structure becomes. Eventually, we can assume that all interior channels are simply filled with a homogeneous screening charge. This is the overlapped DLs model.

Figure 1 illustrates these two extreme cases.

In effect, we can speak of three important regions corresponding to the two simple cases just described as well as a third region of uncertainty that does not fall into either region of simplicity. We can derive an approximate line that separates each of the simple cases from a more complex region of uncertainty.

We can introduce a critical porosity χ_{iso} that determines the applicability of the thin isolated DL model. This critical porosity occurs when the shortest distance between particle surfaces is double the DL thickness and yields the following condition for the validity of the thin isolated DL model:

$$\chi > \chi_{iso} = 1 - \frac{0.52}{\left(1 + \frac{1}{\kappa a_1}\right)^3} \text{and } \kappa a_1 > 10 \tag{11}$$

Similarly, we can introduce a second critical porosity χ_{over} that determines the applicability of the overlapped DLs model. This critical porosity occurs when the distance between particle centers equals the DL thickness and yields the following condition for the validity of the overlapped DLs model:

$$\chi < \chi_{over} = 1 - 4.18(\kappa a_1)^3 \tag{12}$$

Figure 2 illustrates the lines separating these three regions depending on the porosity of the aggregate and the parameter κa_1 for the primary particles.

The double layer contains additional ions. These ions cause extra electric conductivity that is usually referred to as surface conductivity. There is a dimensionless number that characterizes the contribution of the surface conductivity in terms of elec-

(15) Somntag, H.; Shilov, V.; Gedan, H.; Lichtenfeld, H.; Durr, C. J. *Colloid Polym. Sci.* **1986**.
(16) Somntag, H.; Florek, E. H.; Shilov, V. N. *Adv. Colloid Interface Sci.* **1982**, *16*, 37.
(17) Muller, V. M. *Theory of Aggregative Changes and Stability of Hydrophobic Colloids*; Institute of Physical Chemistry: Moscow, 1982.
(18) Lushnikov, A. A.; Piskunov, V. N. *Kolloid Zh.* **1977**, *39*, 857.
(19) Dukhin, A. S. *Kolloid Zh.* **1987**, *5*, 755.

trokinetic effects. It is the so-called Dukhin number *Du*.[20,21] If *Du* is small

$$Du \ll 1 \tag{13}$$

then both electrokinetic and electroacoustic theory are especially simple, as described below.

Acoustics. The main purpose of the acoustic measurement is the determination of the particle size distribution from the experimental ultrasound attenuation α_{exp} measured as a function of ultrasound frequency *f*. To extract this information, we need a theory that would provide a theoretical value of ultrasound attenuation at a given frequency for a particular particle size distribution α_{th} (PSD). We have such a theory that is experimentally verified for a wide range of sizes from 5 nm to 600 μm and solid loads from 1 up to 50% vl. This theory is detailed in ref 22. It takes into account a multitude of mechanisms that cause ultrasound attenuation in heterogeneous systems.

In the case of solid submicrometer particles, only two mechanisms from this multitude are important: viscous drag due to particle motion and intrinsic dissipation in the pure liquid.

In the case of porous particles, one additional mechanism has recently been suggested by O'Brien.[23] It is related to the relaxation of the pressure gradient in the porous particles. The pressure gradient reaches a uniform space distribution inside the porous aggregate if the ultrasound frequency is sufficiently low. Increasing frequency creates lagging of this pressure gradient. When the frequency becomes very large, the pressure gradient inside the pores does not react at all. It is known that a phase lag is associated with energy dissipation. O'Brien presents details of the theory describing this effect.

There is a certain frequency that characterizes this pressure gradient phase lag. The value of this frequency was known prior to O'Brien's work from studies of the oscillating pressure propagation within a single microcapillary.[24,25] There is an expression derived in those papers for the critical time that characterizes this relaxation process τ, which is simply the reciprocal of the critical frequency

$$\tau \cong \frac{a_i^2 \nu}{Kc^2} \tag{14}$$

where the characteristic length is specified as the aggregate radius a_i, ν is the kinematical viscosity, c is the sound velocity, and K is the Darcy constant. The last parameter can be expressed through the aggregate porosity χ and primary particles radius a_1 using the hydrodynamic cell model.[26] This leads to the following expression for the critical time

$$\tau \cong \frac{4\nu k(1-\chi)a_i^2}{c^2\chi a_1^2}[\text{second}] \tag{15}$$

where k is the Koseny–Carman constant (i.e., ~4).[26]

We can use this expression to estimate the importance of this attenuation mechanism in porous silica that is the object of the experiment in this work. It turns out that this additional attenuation is negligible for CMP silica dispersions.

This would reduce the existing theory for calculating the theoretical attenuation frequency spectra of the fumed submicrometer silica down to viscous dissipation. Input parameters should reflect the particular nature of these particles. These input parameters are an essential part of the general principles underlying all macroscopic fitting techniques.

These principles state that the particle size distribution that provides the best theoretical fit to the experimental data represent the particle size distribution of the real heterogeneous system. We can find this best PSD by minimizing the difference between theory and experiment. This would require a search for the minimum of the fitting error function *Err*:

$$Err(\text{PSD}) = \frac{\sum_i |\alpha^i_{expt} - \alpha^i_{th}(\text{PSD})|}{\sum_i \alpha^i_{expt}} \tag{16}$$

There is the danger for all macroscopic fitting techniques that several close minima would exist. This lead to several potential particle size distributions, and we would not know which one is correct. This danger is real for the acoustic attenuation technique as well.

There is only one way to eliminate the possibility of multiple solutions—restrict the number of adjustable parameters. Our experience with the acoustic attenuation technique tells us that we can use a maximum of four adjustable parameters to prevent multiple solutions. Unfortunately in the case of small submicrometer particles with a rather narrow distribution, this number is even less—only two adjustable parameters.

This forces us to use PSD with a predefined shape. The most well known is lognormal PSD. It has only two independent parameters: median diameter (d) and standard deviation (σ). The error function becomes a function of only two parameters for lognormal PSD:

$$Err(d, \sigma) = \frac{\sum_i |\alpha^i_{expt} - \alpha^i_{th}(d, \sigma)|}{\sum_i \alpha^i_{expt}} \tag{17}$$

It is possible to create a very detailed search for the unique minima of this function in the 2D space that would always yield a unique solution, especially for submicrometer particles.

The usual output of this searching procedure is the median particle size, the standard deviation, and the fitting error. The last parameter is very important for judging the reliability of the PSD that is found. Large values of the fitting error would indicate problems with the theoretical fit. This is a flag that the PSD might not be correct because of the mistaken model assumption or input parameters.

A theoretical description of sound propagation through the heterogeneous system begins with postulating the existence of the dispersed phase and the dispersion medium. It is an absolutely essential step. No theory of this phenomenon is possible without introducing the notion of the dispersed phase.

The dispersed phase is a collection of finitely divided material that is spread in the homogeneous and continuous dispersion medium. We use term "particle" to refer to these elements of the

(20) Lyklema, J. *Fundamentals of Interface and Colloid Science*; Academic Press: London, 2000; Vol. 1.

(21) *Measurement and Interpretation of Electrokinetic Phenomena*; IUPAC Technical Report; International Union of Pure and Applied Chemistry; *Pure Appl. Chem.* **2005**, *10*, 1753–1805.

(22) Dukhin, A. S.; Goetz, J. P. *Ultrasound for Characterizing Colloids: Particle Sizing, Zeta Potential, Rheology*; Elsevier: Amsterdam, 2002.

(23) O'Brien, R. W. *J. Phys. Chem. Chem. Phys.*, in press, 2006.

(24) Dukhin, S. S.; Kovalchuk, V. I.; Fainerman, B. B.; Miller, R. *Colloids Surf.* **1998**, *141*, 253–260.

(25) Dukhin, S. S.; Mishchuk, N. A.; Fainerman, V. B.; Miller, R. *Colloids Surf., A* **1997**, *138*, 51.

(26) Happel, J.; Brenner, H. *Low Reynolds Number Hydrodynamics*; Prentice-Hall: Englewood Cliffs, NJ, 1965.

dispersed phase. Particles might have different chemical natures, but for most scientific purposes, we are dealing with just a single dispersed phase.

We would like to stress here that the introduction of these notions is required for the theoretical description all macroscopic phenomena in heterogeneous systems, such as light scattering, ultrasound attenuation, rheology, conductivity, dielectric permittivity, and so forth.

As the next step, we assign certain properties to the dispersion medium and the dispersed phase. Here we mention only those parameters that are important for describing ultrasound attenuation by the dispersion of submicrometer rigid particles in a Newtonian liquid.

For the dispersion medium, we need the density ρ_m and dynamic viscosity η_m. In addition, we need the acoustic properties of the liquid, which include the speed of sound c_m (m/s) and the intrinsic attenuation of water α_m[1] (dB/cm/MHz). The speed of sound is almost independent of the frequency of ultrasound. However, intrinsic attenuation of the Newtonian liquid is a linear function of frequency in our units, as it shown by Stokes 150 years ago.[22] The known frequency dependence allows us to use just one number to characterize the intrinsic attenuation of the dispersion medium. We use attenuation at 100 MHz as this number.

For particles of the dispersed phase, we need just density ρ_p.

In addition, all macroscopic effects would depend on the volume fraction of the dispersed phase (φ_p) or the weight fraction (w_p).

The introduction of the particle density and the dispersed phase volume fraction is intuitively obvious, but it is not trivial.

First, we assume that each particle fills a certain volume of space. This indicates that there is a well-defined border between a solid particle and the liquid dispersion medium. In the case of homogeneous particles, the position of this border was defined by Gibbs a century ago.[20]

However, in the case of composite particles the location of the border between particles and the liquid is not well defined, and unfortunately it is not unique. An interpretation of the macroscopic phenomena demands the introduction of this border. It would be impossible to build a theory without this step.

An introduction of the well-defined particle volume is also required for linking particles properties with known properties of the solid material of the dispersed phase. We do know and can easily measure with a pycnometer the density of the solid material that makes the particle ρ_s, weight fraction w_s, and volume fraction φ_s of solids in the liquid.

This model also requires information on the primary size. It is possible to use this parameter as adjustable instead of the standard deviation. This means that for the purpose of fitting the attenuation spectra we consider a monodisperse collection of aggregates with the same size and the same primary size. These two numbers are adjustable parameters in eq 17 instead of the median size and standard deviation of the lognormal PSD.

Electroacoustics. Debye[27] first predicted an electroacoustic effect 70 years ago. In either electrolyte solutions or dispersions, the effect is related to a coupling between electrodynamic and mechanical phenomena. For instance, the transmission of ultrasound through an electrolyte solution or dispersion generates a current, which is usually referred to as an ion/colloid vibrational current. Commercial instruments used to measure this effect are available for the purpose of determining the ζ potential of dispersed particles in liquids.

Experimental output of the electroacoustic measurement is the colloid vibrational current (CVI) magnitude and phase. They are usually converted to the dynamic electrophoretic mobility and ζ potential, which are considered to be outputs of the electroacoustic technique. This conversion procedure requires a proper theory. There are several versions of electroacoustic theory. Here we use two of them.

The simplest version of electroacoustic theory is valid for sufficiently small particles with thin DL and negligible surface conductivity, when conditions 10 and 13 are valid. Electroacoustic theory reduces for this case to the Smoluchowski theory for dynamic mobility, as shown in ref 28. This Smoluchowski version of the electroacoustic theory yields the following expression for CVI

$$\frac{\mathrm{CVI}_{\omega\to 0}}{\nabla P} = \frac{\epsilon_m \epsilon_0 \zeta \varphi K_s}{\eta K_m} \frac{(\rho_p - \rho_s)}{\rho_s} \tag{18}$$

where P is pressure in the sound wave, ϵ_m and ϵ_0 are the dielectric permittivities of the media and vacuum, φ is the volume fraction of the dispersed phase, η is dynamic viscosity, ρ_p, ρ_m, and ρ_s are densities of the particle, media, and dispersion, and K_s and K_m are the conductivities of the system and media.

Expression 18 also neglects the inertia of the particles. This assumption is valid if particles are sufficiently small for a given frequency.

In addition to the Smoluchowski theory, there is a version of the theory that still assumes a thin double layer but takes into account the surface conductivity effect. It is derived in refs 28 and 29 and given in ref 22:

$$\frac{\mathrm{CVI}}{\nabla P} = \frac{2\epsilon_0 \epsilon_m \zeta \varphi (\rho_p - \rho_s)}{3\eta \rho_s} \sum_{i=1}^{N} G(s_i, \varphi_i)(1 + F_i(Du_i, \phi)) \tag{19}$$

Values of functions G and F are on p 171 in ref 22.

This equation contains two unknown parameters: the ζ potential and Du. We can use a standard double-layer model to relate Du to the ζ potential

$$Du = \frac{\exp\left(\frac{F\zeta}{RT}\right)}{\kappa a} \tag{20}$$

where F is the Faraday number, R is the gas constant, and T is the absolute temperature.

Combining eqs 19 and 20, we can calculate the ζ potential from the measured CVI magnitude and then calculate the Dukhin number.

All of these calculations also require the density and volume fractions of the dispersed phase. We take these numbers for different particle models presented above.

Conductivity. There is a well-known theory that describes the conductivity of liquids on the megahertz range of ultrasound frequencies. It is the Maxwell−Wagner−O'Konski theory.[30−32]

In this particular case, we can use a low-frequency limit of this theory.[29] This simplification is justified by the fact that the frequency of the measurement is much smaller than the Maxwell−Wagner frequency for the observed range of conductivities. The

(27) Debye, P. *J. Chem. Phys.* **1933**, *1*, 13−16.

(28) Dukhin, A. S.; Shilov, N. V.; Ohshima, H.; Goetz, P. J. *Langmuir* **1999**, *15*, 6692−6706.

(29) Dukhin, A. S.; Shilov, V. N.; Borkovskaya, Y. *Langmuir* **1999**, *15*, 3452−3457.

(30) Maxwell, J. C. *Electricity and Magnetism*; Clarendon Press: Oxford, England, 1892; Vol. 1.

(31) Wagner, K. W. *Arch. Elektrotech.* **1914**, *2*, 371.

(32) O'Konski, C. T. *J. Phys. Chem.* **1960**, *64*, 605−612.

measurement frequency is 3 MHz, whereas the Maxwell−Wagner frequency for 0.5 S/m conductivity is about 115 MHz.

There is a simple expression for the low-frequency conductivity derived on the basis of both Maxwell−Wagner theory[30,31] and the Shilov−Zharkikh cell model:[33]

$$\frac{K_s}{K_m} = \frac{1 + Du - q(1 - 2Du)}{1 + Du + 0.5q(1 - 2Du)} \tag{21}$$

There is a parameter in this expression that determines the contribution of the particle surface conductivity—*Du*, the so-called Dukhin number.[20,21] We can use experimental conductivities to calculate the values of this parameter in both models, separate particles and fractal.

It is important to mention that the *Du* parameter not only reflects the surface conductivity for nonconducting particles but also characterizes in the case of conducting particles the contribution of the internal particle conductivity to the conductivity of the dispersion. For conducting particles, we can use the following equation for *Du*

$$Du = \frac{K_p}{2K_m} \tag{22}$$

which simply converts eq 21 to the Maxwell−Wagner equation for conducting particles.

This means that values of *Du* calculated for the fractal model reflect not only the particle surface conductivity but also the internal conductivity of the aggregate.

We also use the conductivity to estimate the double-layer thickness κ^{-1}. There is an expression that relates this parameter to the conductivity and dielectric permittivity of the media plus an effective diffusion coefficient.[22] It is derived from the two interpretations that exist for the Maxwell−Wagner frequency, ω_{MW}. From DL theory, it is the frequency of the DL relaxation to the external field disturbance. From general electrodynamics, it is the frequency at which active and passive currents are equal. Thus, ω_{MW} can be defined by two expressions:

$$\kappa^2 D_{eff} = \omega_{MW} = \frac{K_m}{\epsilon_0 \epsilon_m} \tag{23}$$

We assume that the effective diffusion coefficient in water is 10^{-5} cm^2/s. This assumption allows us to estimate the κa values.

Instruments

Altogether we use a light-based instrument, an ultrasound-based instrument, a TEM, a conductivity meter.

The light-based instrument was a Malvern Zetasizer 3000HS$_A$. The instrument measures particle size using the light-scattering technique known as photon correlation spectroscopy (PCS), which is an absolute method based on Brownian motion. The laser source light is oriented at 90° with respect to the detector. The calibration was checked with 50 nm latex standard (50 nm +2.0 nm) from Duke Scientific (cat. no. 3050A; exp date, Mar 07) of Palo Alto, CA. Two drops of this standard was added to a $^3/_4$ full cuvette filled with 10 mM sodium hydroxide solution. The cuvette was capped and shaken to ensure proper mixing. The cuvette containing the standard was then placed in the instrument and analyzed to check the calibration. A mean value of 50.3 nm was obtained for the 50 nm calibration particles. The process was repeated for the silica samples using two drops of concentrate that was diluted with the same 1 mM sodium chloride solution.

(33) Shilov, V. N.; Zharkih, N. I.; Borkovskaya, Y. B. *Kolloid J.* **1981**, *43*, 434−438.

The ultrasound instrument used is a Dispersion Technology model DT-1200, which contains both acoustic and electroacoustic sensors as well as a built-in conductivity probe. Details are available at www.dispersion.com and in ref 22.

The main purpose of the acoustic measurement is the determination of ultrasound attenuation at various frequencies. The DTI acoustic sensor works on the "transmission" principle. A piezoelectric transducer converts an input electrical tone burst to an ultrasound pulse of a certain frequency and intensity I_{in} and launches it into the sample. The intensity of this pulse decreases as it passes through the sample as a result of the interaction with the fluid. A second piezoelectric transducer converts this weakened acoustic pulse with intensity I_{out} back to an electric pulse and sends it to the electronics for comparison with the initial input pulse. The total loss and time delay from the input to output transducer for each frequency and gap can be considered to be the raw data from which further interpretation is made.

It is convenient to present these raw data in terms of an attenuation coefficient α_{expt} defined as

$$\alpha_{expt} = \frac{10}{f(\text{MHz})L(\text{cm})} \log \frac{I_{in}}{I_{out}} \tag{24}$$

where f is the frequency of the pulse and L is the distance between the transmitter and receiver.

The typical frequency range for attenuation measurement is 1−100 MHz, and the typical gap range is from 0.3 to 20 mm. The precision of the measurement is 0.01 dB/cm/MHz, and the maximum attenuation measured with DTI instruments is limited by 20 dB/cm/MHz.

The attenuation measurement is closely linked to the speed of sound measurement. One needs to know the speed of sound for sampling pulses at the proper time. A DT-1200 acoustic sensor was used to measure the speed of sound c using the time-of-flight method. The instrument measures the delay time between emitting and receiving the pulse t for a set of gaps. The speed of sound is obtained from the linear regression $c = L/t$. It is usually done at a single frequency.

The attenuation frequency spectrum is a source of information for calculating the particle size distribution using theory as described above in the Theory, Acoustics section. DTI software allows the testing of different particle models with particular sets of input parameters, as described above in the section Theory, Models of Particles.

The DT-1200 electroacoustic sensor employs an effect predicted by Debye[27] 70 years ago. In either electrolyte solutions or dispersions, the effect is related to coupling between electrodynamic and mechanical phenomena. For instance, the transmission of ultrasound through an electrolyte solution or dispersion generates a current that is usually referred to as an ion/colloid vibrational current. Commercial instruments used to measure this effect are available for the purpose of determining the ζ potential of dispersed particles in liquids. We use the electroacoustic sensor of the DT-1200 as our zeta potential probe. Inside the probe, there is a piezoelectric transducer that converts an electrical tone burst signal to a sound pulse that is then transmitted to the front face of the probe and into the colloid. The colloid vibrational current (CVI) between a central gold electrode and a surrounding annular electrode is measured electronically. This signal is then converted into a ζ potential of the particles using appropriate equations, as described above in the section Theory, Electroacoustics.

The frequency of the measurement is 3 MHz by default, but the user can change it. The number of collected pulses is automatically adjusted to improve the signal-to-noise ratio. The software uses the reflection inside the probe for the automatic calibration of the pulse intensity. The measurement of the DTI standard (10 wt % silica Ludox) calibrates the electric field geometry. There are several detailed studies of this material overviewed in ref 22. An acoustic measurement yields 29 nm particles with the precision of a fraction of a nanometer. An independent microelectrophoretic measurement of the supernatant diluted system and assuming the use of Smoluchowski theory give an electrokinetic potential of −38 mV.

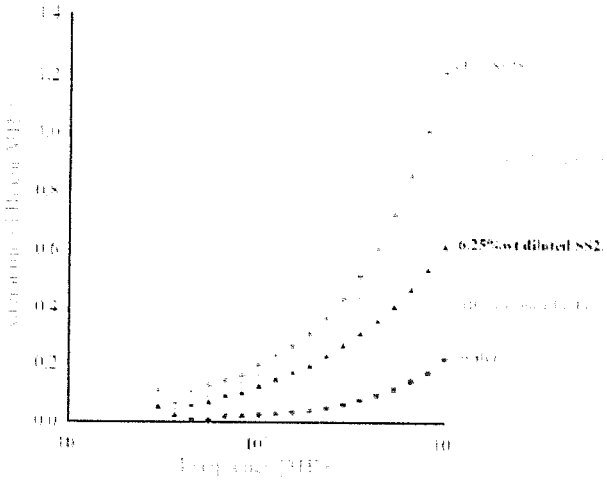

Figure 4. Attenuation spectra measured for silica Semisperse SS25 at the original weight fraction and several dilutions. For comparison, we also show the attenuation of the colloidal silica Ludox TM with a size of about 30 nm. The attenuation of pure water is the background for calculating the particle size distributions.

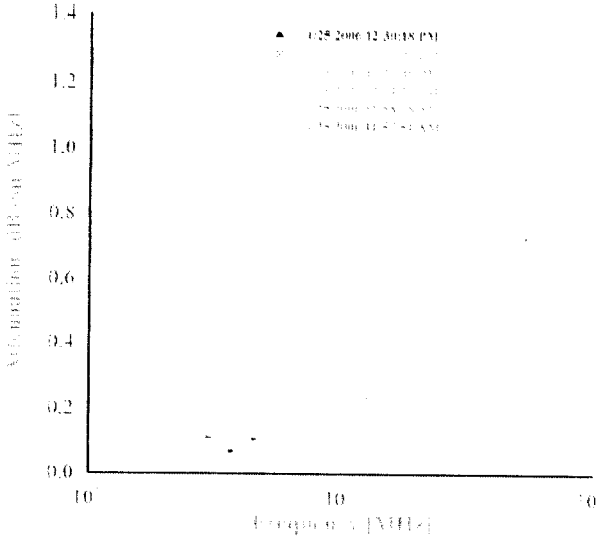

Figure 5. Reproducibility of the attenuation measurement with DT-1200.

The conductivity probe of the DT-1200 functions at a 3 MHz default frequency. This eliminates the effect of electrode polarization and allows the use of a simple two-electrode design. The precision of the measurement is about 1%, and the probe must be calibrated with conductivity standards.

Materials

We used a commercial CMP material manufactured by Cabot Microelectronics Corporation and referred to as Semisperse SS25. It is a polishing slurry made from fumed silica. This fumed silica is composed of aggregated particles and is known for its fractal structure. No sample preparation was involved for the first set of acoustic, electroacoustic, or conductivity measurements: the samples were measured neat.

We also made a second set of measurements on samples that were in fact diluted 2:1 with distilled water.

To obtain the properties of the equilibrium media, we centrifuged both the neat sample and the diluted sample to obtain a supernatant devoid of particulates. This supernatant provided information on the conductivity of the equilibrium media.

Experimental and Calculated Data

We present results obtained with different techniques in this section. The next section presents a cross comparison of these results.

Acoustics. Experimental attenuation spectra measured for silica samples are shown in Figure 4. We show results for some other systems, including pure water, for comparison. Figure 5 illustrates the reproducibility of the attenuation measurement. We can use these attenuation spectra to calculate particle size distributions (PSD) for all three models: separate particles, porous particles, and fractal particles.

These calculations are simplified because we can consider the pressure gradient to be quasistationary inside the particles. Expression 15 yields the value of the critical frequency for the pressure relaxation inside the particles. In the given case of the fractal silica with aggregate and particle sizes of about 170 and 30 nm, respectively, this frequency equals 4×10^3 MHz. It is much higher than the frequency of the measurement. That is why we can ignore the additional attenuation mechanism predicted by O'Brien[25] and take into account only the viscous drag of the particles.

An application of the porous particles model requires information on porosity, but it is unknown. However, we can run a set of calculation for several different porosities and compare our results with independent methods. Figure 6 shows the median size for different porosities and the fitting error. It also presents the size range coming from independent techniques. It is seen that this theory yields results that are consistent with independent methods if we assume that the porosity of the particles is between 40 and 50%.

This means that half of the particle hydrodynamic effective volume is filled with water. The effective density of the aggregate is about 1.6 g/cm^3.

It is interesting that the fitting error goes up sharply at higher porosities. This means that this model will not be able to describe ultrasound attenuation and other hydrodynamic effects at higher porosities, above 50%.

Unfortunately, we cannot determine the porosity from the acoustic spectroscopy. Consequently, we cannot point toward one particular aggregate size using this model.

Fortunately, the fractal model resolves this problem. Instead of porosity, the fractal number plays the role of unknown input parameter in this case. Again, we can calculate the aggregate size for all possible values of the fractal number. These data are shown in Figures 7 and 8. The size of the primary particles shown in these Figures is the second parameter calculated as adjustable from attenuation spectra, as described in the section Theory, Acoustics.

It is clearly seen that size of the aggregate is practically independent of the fractal number below 2.8. We can use practically any value of the fractal number to fit the experimental attenuation and get the correct aggregate size.

What is important is that this size value agrees well with independent light-scattering measurements (Figure 10).

Image Analysis. Figure 9 shows an example of an image of a fumed silica aggregate. The mass-weighted primary particle diameter for this grade of fumed silica is approximately 28 nm, as measured by transmission electron microscopy. This photograph and information were provided by Dr. David Boldridge.

Light Scattering. Figure 10 illustrates the particle size distribution measured with a Malvern PCS light-scattering instrument. It reports the particle size distribution on a volume

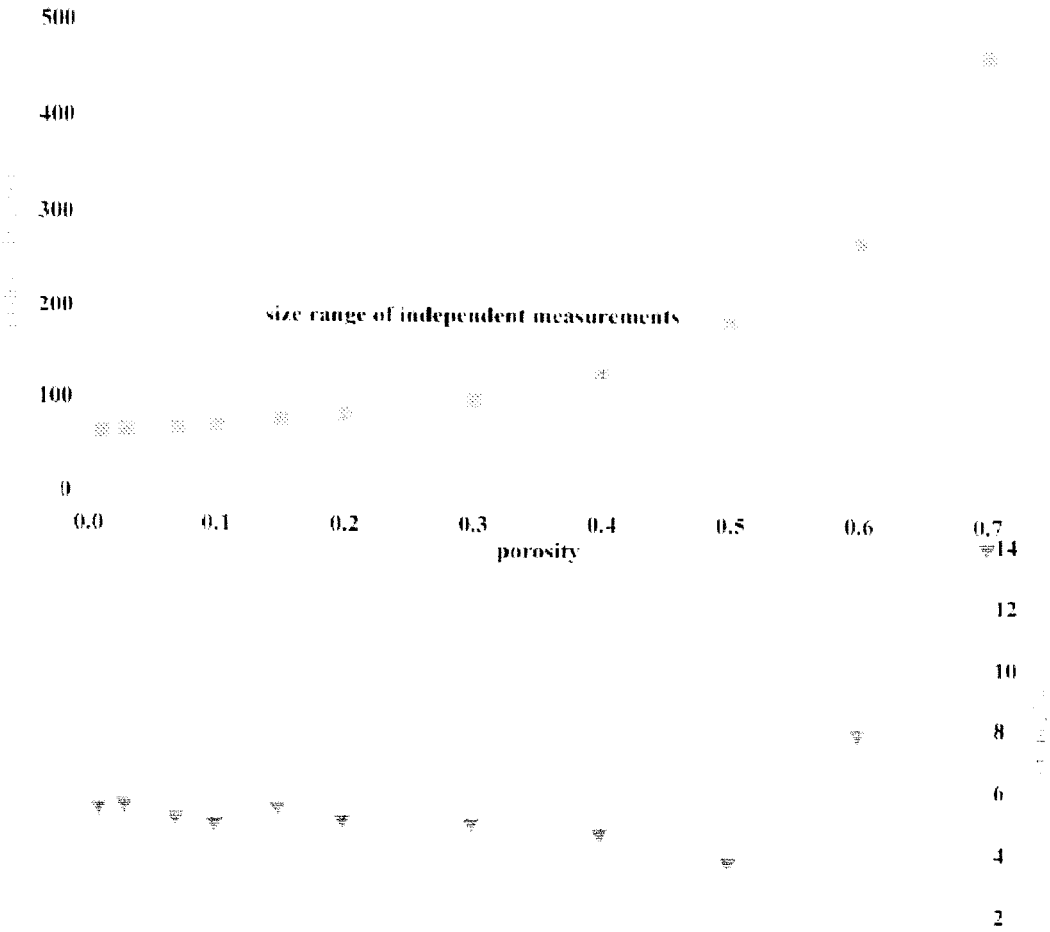

Figure 6. Aggregate sizes and theoretical fitting error calculated for the original Semisperse SS25 silica slurry with the porous particle model for different values of the aggregate porosity.

basis. Values of the mean particle size are reported in Table 1 for both original Semisperse SS25 and the orignal solution diluted 2-fold.

There is one important assumption employed for calculating the particle size distribution in this method. Particles are assumed to be hard spheres. Theory does not take into account possible liquid motion inside the aggregates or deviation from the boundary slip condition on the surface of the aggregate. The density of neither the particles nor the aggregates affects the calculated size distribution. In this sense, this model is similar to the fractal model.

Conductivity. Measured values of conductivity for the silica samples and their supernatants are given in Table 2. Theory presented in the section Theory. Conductivity allows us to calculate the value of the Dukhin number, Du, and the relative double-layer thickness, κa. These values are shown in Table 2 as well.

Electroacoustics. Table 2 presents values of the ζ potentials and Du numbers calculated from the measured CVI using different models of the silica particles. These calculations require the density and volume fraction of the dispersed phase. We take these numbers from the acoustic data, listed in Table 1 for both the separate particles and fractal models.

There is one more parameter required for these calculations—the particle size. We use the value given in the section Image Analysis for the size in the separate particles model. It is 28 nm. In the fractal model, we use the size of the fractal aggregate coming from acoustics (Table 1). This value agrees well with light scattering.

Values of the dispersion and media conductivities come from the conductivity experiment presented in Table 2.

Discussion

Using several techniques to characterize the silica slurry, we have achieved the possibility of comparing their results and deriving some conclusions from this comparison.

First, there is good agreement between the aggregate size provided by acoustics with the fractal model and light scattering (Table 1).

At the same time, the separate particles model fails completely for sizing.

This is an indication that advection hydrodynamic flow is not that important for calculating an adequate particle size from acoustics attenuation spectra.

This particle size has a well-defined meaning. It is the diameter of a sphere that dissipates as much energy moving relative to the liquid as real silica fractal aggregates. This diameter is usually referred to as the equivalent hydrodynamic sphere diameter.

In the case of electrokinetics situation the reverse is true: the fractal model fails, but the separate particles model succeeds very well. We come to this conclusion by comparing values for the Dukhin number coming from conductivity and CVI measurements (Table 2).

What is the reason for this difference? Image analysis clearly and unambiguously tells us that these silica particles are actually

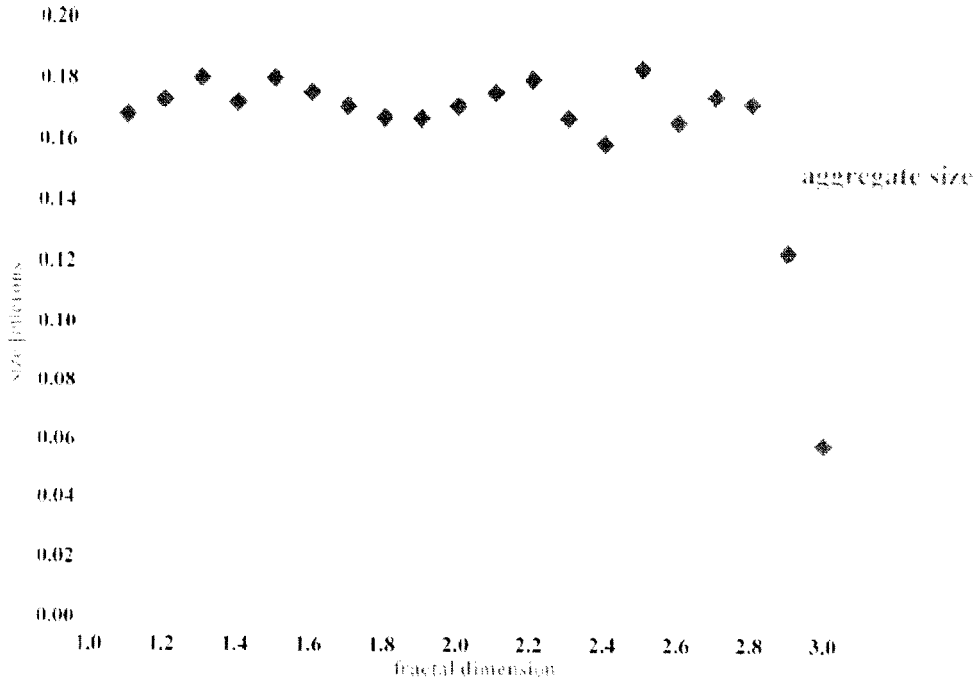

Figure 7. Aggregate and primary sizes calculated for the original Semisperse SS25 silica slurry with the fractal particle model for different values of the fractal dimension.

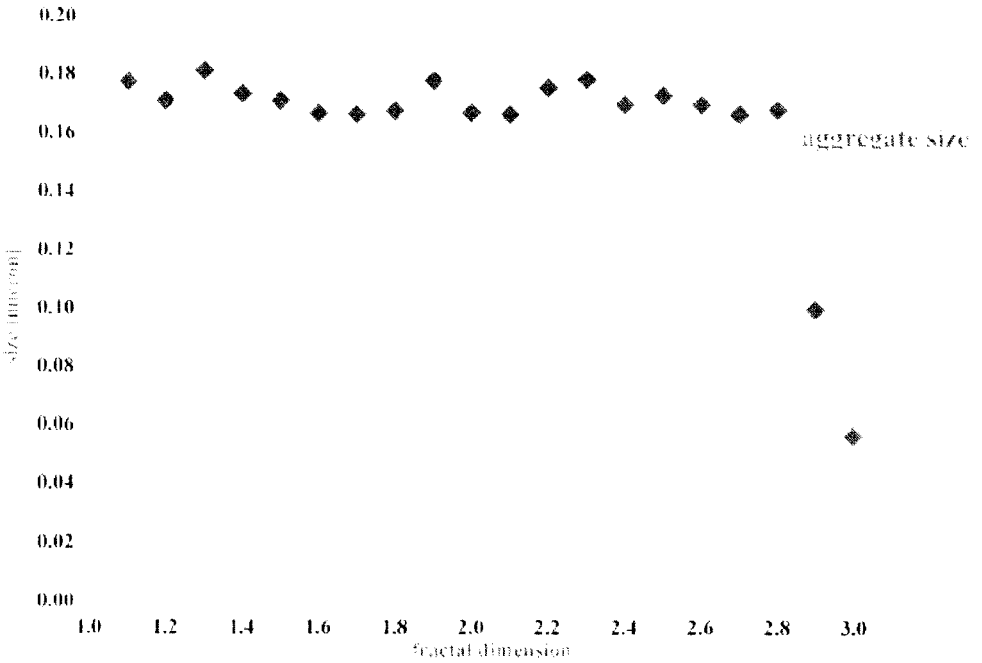

Figure 8. Aggregate and primary sizes calculated for the 2-fold diluted Semisperse SS25 silica slurry with the fractal particle model for different values of the fractal dimension.

fractal aggregates. Acoustics requires this information for a proper interpretation of the experimental data. An alternative porous particle model is inconclusive because we do not know the actual porosity of the particles. Consequently, we cannot come up with a certain aggregate size. Various values of the porosity would yield different size, as shown in Figure 6.

The fractal particles model turns out to be superior for acoustic sizing. It yields the size of the aggregate independently of the fractal number. The fractal number determines the density and weight fraction of aggregates but not their size. Most importantly, we can ignore advection when calculating the size using this model.

In contrast, the interpretation of the electrokinetic phenomena requires one to ignore the organization of the particles in aggregates. This occurs because we are dealing with a system that is close to the Smoluchowski range.

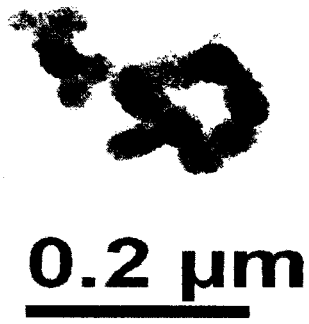

Figure 9. Image of the silica aggregate.

There are two requirements that determine the Smoluchowski range: thin DL (eq 10) and negligible surface conductivity (eq 13). Both requirements are almost valid for this silica dispersion.

According to the data in Table 2, the κa parameter is about 10. It is in the range where DL is still thin compared to the primary particle size but deviation from the Smoluchowski theory becomes measurable.

The situation with the other parameter—the Dukhin number—is similar. According to the conductivity measurements (Table 2), it is about 0.2. This value much smaller than 1, but surface conductivity becomes a measurable factor.

It seems that this silica dispersion is just beyond the validity of the Smoluchowski law. This means that some features of the Smoluchowski law are still valid for this system.

Smoluchowski theory has a wonderful feature—it predicts that electrophoretic mobility is independent of the shape of solid particles when this theory is valid. A single silica particle would move in an electric field with the same speed as a fractal aggregate built from many such particles.

Will this independence with respect to shape hold when we use ultrasound as a driving force, instead of the electric field? On one side, it must because of the Onsager principle.[14]

It turns out that it does as a result of the Onsager principle. It is shown in the Appendix that the Onsager principle holds for electroacoustics of porous aggregates because the pressure gradient can penetrate into the porous particle even when liquid flow through it is practically zero. This pressure gradient creates a liquid velocity gradient in the vicinity of the pore walls. Ultrasound-induced current depends only on the gradient of the liquid velocity, not on the velocity itself.

Here we can simply conclude that the separate particles model succeeds because we are dealing with a system in close proximity to the Smoluchowski regime, where the shape factor is not important for electrokinetics.

Conclusions

Acoustic spectroscopy yields sufficient information to calculate the size of the fractal aggregates. The basis of this calculation constitutes the simplest fractal particle model that neglects advection. It proves to be adequate for results of both acoustic spectroscopy and light scattering when particles are sufficiently small. Within the constraints of this fractal particle model, the measured size of the fractal aggregates is not dependent on the fractal dimension.

This simple fractal particle model does not work for electrokinetic phenomena of porous particles. It contradicts the essential consequence of the Onsager principle of the symmetry between electric and pressure driving forces. This contradiction can be resolved if one takes into account the internal liquid flow. It arises within the porous particles even with low porosity as a result of the pressure gradient that penetrates into the particles at any porosity. The fractal particle model with no advection ignores any internal irreversible phenomena within the aggregate. Therefore, it is inapplicable to electrokinetic and electroacoustic phenomena. We proved this conclusion by comparing the results of conductivity and electroacoustic measurements.

However, the separate particles model that completely fails for particle sizing by acoustics succeeds for electrokinetic phenomena. It happens in this particular case when double layers are thin and the surface conductivity is relatively low. These two conditions indicate that this particular silica dispersion is in close proximity to the Smoluchowski range. Smoluchowski theory predicts the independence of the electrokinetic and electroacoustic effects with respect to the shape of the particles, when it is valid. Separate particles move with the same dynamic electrophoretic mobility as fractal aggregates if the electric field is a driving force. In the case of ultrasound as a driving force, Smoluchowski theory should retain its features according to the Onsager principle, as shown in the Appendix. The independence of the dynamic mobility with respect to particle shape is the reason that the separate particles model succeeds for these small silica particles.

Acknowledgment. We express our gratitude to Dr. David Boldridge of Cabot Microelectronics Corporation for providing data on the image analysis of this fumed silica.

Appendix: Onsager Principle and Direct Calculations of Electroacoustic Phenomena for Porous and Fractal Particles

We have concluded that agreement between microelectrophoresis and electroacoustics can be achieved when we use the density of the solid material instead of the average aggregate density to calculate the ζ potential from CVI. This conclusion requires an explanation of how streaming current develops inside the aggregate despite its low hydrodynamic permeability that prevents almost any hydrodynamic flow inside. This Appendix offers such an explanation.

The basis of our conclusion is expression 12 for CVI. It has been derived from the Smoluchowski law using Onsager's symmetry relationship. It inherits a wide validity range that is peculiar for Smoluchowski law. It is valid for any particle shape and concentration. For the case of a dilute system when the density and conductivity of the dispersion are almost identical to the same properties of the media, eq 12 reduces to the following:

$$\frac{\mathrm{CVI}_{\omega\to 0}}{\nabla P} = \frac{\epsilon_m \epsilon_0 \zeta \varphi}{\eta} \frac{(\rho_p - \rho_m)}{\rho_m} \qquad (1A)$$

Both eqs 11 and 1A contain the density of the solid material independently of the shape of the particles. This allows us to model the aggregate as a single particle with a very complex shape but with the density of the solid material only. This leads to the validity of the separate solid particles model for describing electroacoustics in the aggregated dispersions when Smoluchowski's law is valid.

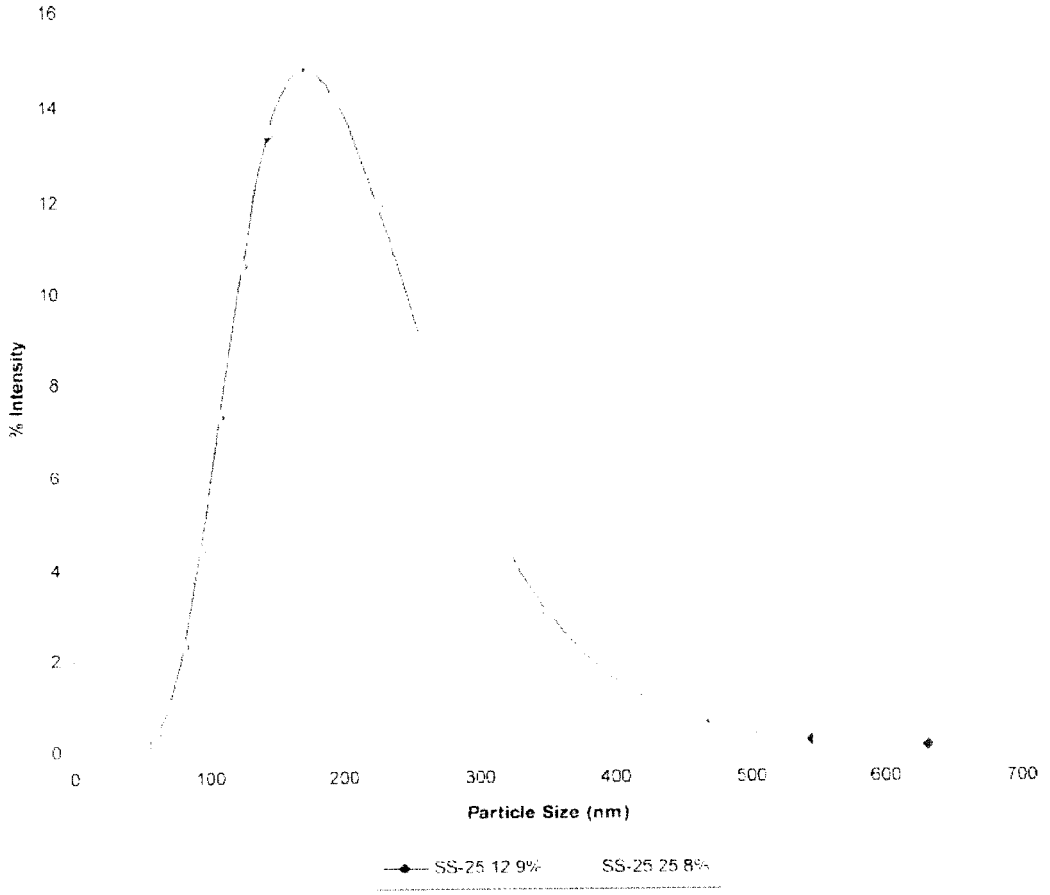

Figure 10. Particle size distribution obtained on a Malvern light-scattering instrument.

Table 1. Median Particles Sizes and Other Parameters Characterizing the Original and 2-Fold Diluted Silica Semisperse SS25 Dispersion within the Scope of the Two Different Models of the Dispersed Phase[a]

			acoustic spectroscopy			
	light scattering		separate particle model		fractal particle model	
	SS25	diluted 1:1	SS25	diluted 1:1	SS25	diluted 1:1
aggregate size, nm	188.2	186.8	58 ± 0.7	55 ± 0.2	172 ± 5	171 ± 4
density particles			2.2	2.2	1.58 ± 0.01	1.44 ± 0.01
volume fraction of the dispersed phase			13.3	6.7	26.7 ± 0.5	16.1 ± 0.3

[a] In the case of the fractal model, the density and volume fraction of the dispersed phase are calculated from the acoustic attenuation spectra. In the case of the separate particles model, these parameters are assumed as being known independently.

However, this is not the directly derived result. It follows from the Onsager relationship but not from the direct analysis of the electroacoustic phenomena inside and outside the aggregates. That is why it remains unclear as to how interior diffuse layers inside the almost nonpenetrable hydrodynamically aggregate move relative to particles and contribute to CVI.

To resolve this seemingly paradoxical conclusion, we perform direct calculations of the hydrodynamic and electric field generated by ultrasound inside the aggregate. The aggregate and surrounding liquid move with acceleration in the ultrasound wave. This generates an inertia force, which in turn induces a pressure gradient ∇p_{ef}. This pressure gradient is responsible for the liquid flow inside even dense aggregates.

We can derive an expression for ∇p_{ef} using the equivalency between inertia and gravity. We can introduce a homogeneous gravity field with acceleration β that is assumed to be equal to the acceleration generated by inertia forces in the ultrasound wave. This gravity would generate a homogeneous hydrostatic pressure gradient $\nabla p_m = -\rho_m \beta$ in the liquid and $\nabla p_p = -\rho_p \beta$ in the particles. The local acceleration in the ultrasound wave can be presented as the ratio of the pressure gradient in this wave ∇p to the density of the dispersion ρ_s:

$$\beta = \frac{1}{\rho_s}\nabla p$$

This leads to the following expressions of the pressure gradients in the liquid and in the particles:

$$\nabla p_m = -\frac{\rho_m}{\rho_s}\nabla p$$

$$\nabla p_p = -\frac{\rho_p}{\rho_s}\nabla p$$

Let us consider the balance of force exerted on the particles in some volume element δV, where they take a volume $q\,\delta V$ and

Table 2. Summary of the Conductivity and Electroacoustic Measurements of the Original CMP Slurry Semisperse SS25 and the Slurry Diluted 2-Fold with Distilled Water

	separate particles model		fractal particle model	
	original SS25	diluted 2-fold	original SS25	diluted 2-fold
conductivity of dispersion, S/m	0.522	0.288	0.522	0.288
conductivity of supernatant, S/m	0.577	0.301	0.577	0.301
volume fraction of dispersed phase, $\%_a$	13.3	6.7	26.7	16.1
Du from conductivity	**0.206**	**0.207**	**0.339**	**0.371**
median diameter for calculating z_{eff} (nm)	28	28	170	170
density of particles	2.2	2.2	1.58	1.44
Ka	8.5 ± 0.003	6.4 ± 0.002	51.7	38.8
ζ_{eA} – Smoluchowski (mV)	−33.1 ± 0.19	−33.3 ± 0.13	−35.0 ± 0.23	−34.1 ± 0.13
ζ_{eA} – advanced (mV)	−45.6 ± 0.3	−50.3 ± 0.21	−52.7 ± 0.42	−43.4 ± 0.24
Du from electroacoustics	**0.195**	**0.260**	**0.053**	**0.065**

the residual volume $(1 - q)\delta V$ belongs to the liquid. There are pressure forces applied to the interior and exterior of the interface: $q\delta V\nabla p_p = q\delta V\rho_p\beta$ and $-q\delta V\nabla p_m = -q\delta V\rho_m\beta$, respectively. The sum of these forces is not zero when ρ_p differs from ρ_m. This summary force generates relative motion between the liquid and particles, which is described by the coupled phase model (refs 34 and 35). If we select particles as a fixed frame of reference, then the motion of the liquid can be described as filtration through the particle diaphragm under the influence of the effective pressure gradient ∇p_{ef} (ref 28). This relative motion is quasi-stationary at low frequencies, and ∇p_{ef} equals

$$\nabla p_{ef} = \frac{q(\rho_p - \rho_s)}{\rho_s}\nabla p$$

In the case of a dilute system, when $\rho_s \approx \rho_p$, the last expression becomes the following:

$$\nabla p_{ef} = \frac{q(\rho_p - \rho_m)}{\rho_m}\nabla p \qquad (2A)$$

This expression indicates that the effective pressure gradient calculated per unit volume fraction in dilute systems is independent of their relative positions. This means that the aggregate with a volume V_A and a volume fraction of solids q_A *would* experience the same effective pressure force $q_A\nabla p_{efA}V_A$ as the total force acting on the separate particles that build this aggregate. The last one should be calculated by assuming that these particles are spread homogeneously with an average volume fraction q in the larger volume $V = V_A q_A/q$ and experience the average pressure gradient ∇p_{ef}

$$\nabla p_{efA}V_A = \nabla p_{ef}\frac{V_A q_A}{q}$$

This yields the following expression for the effective pressure gradient inside the aggregate

$$\nabla p_{efA} = \nabla p_{ef}\frac{q_A}{q} \qquad (3A)$$

We can conclude that the ultrasound causes liquid filtration through the aggregate by means of the oscillating pressure gradient that is proportional to the volume fraction of particles in the aggregate. Aggregate hydrodynamic resistance increases much faster than linearly with increasing particle volume fraction. Consequently, the liquid flow rate through the aggregate decreases rapidly with increasing particles volume fraction.

Nevertheless, the streaming current inside the aggregate would not decrease, unless condition 10 is valid. It is the fact that must be taken into account to explain it.

First of all, liquid flow inside the thin diffuse layer forms in close proximity to the surface. Its rate relative to the particle has only the tangential component v_t, which may be represented as $v_t = \partial v_t/\partial x\ x$, where x is the distance from the surface. Consequently, the electric streaming current generated by the liquid flow inside the thin diffuse layer is not proportional to the liquid flow rate through the aggregate, which diminishes for dense aggregates. Instead, it is proportional to the normal derivative of the tangential flow velocity, $\partial v_t/\partial x$. This conclusion follows directly from the well-known expression for the surface streaming current density (per unit length of the contour traced at the surface and perpendicular) in the thin DL:

$$I_s = -\epsilon_m\zeta\frac{\partial v_t}{\partial x} \qquad (4A)$$

The same normal derivative determines a local viscous stress that the aggregate surface exerts on the liquid:

$$\tau_s = -\eta\frac{\partial v_t}{\partial x} \qquad (5A)$$

Combining eqs 4A and 5A, there is geometrical similarity between surface streaming current in the thin DL and viscous stresses on the surface between the aggregate and liquid:

$$I_s = \frac{\epsilon_m\zeta}{\eta}\tau_s \qquad (6A)$$

Let us consider now the balance of forces that act on the liquid within a small volume element. This element is a cylinder that is oriented perpendicular to the ultrasound wave vector and has a height δz that is much smaller than the cylinder diameter. This element is a cylinder of height δz that is much smaller than the cylinder diameter. The base of the cylinder is oriented perpendicularly to the ultrasound wave vector.

There are two forces acting on the liquid within the cylinder: the viscous force δF_{visc} generated by the particle surface and pressure force δF_p caused by neighboring liquid layers. The total

(34) Harker, A. H.; Temple, J. A. G. *J. Phys. D.: Appl. Phys.* **1998**, *21*, 1576–1588.

(35) Gibson, R. L.; Toksoz, M. N. *J. Acoust. Soc. Am.* **1989**, *85*, 1925–1934.

force acting on the liquid inside the cylinder equals the sum of these two forces δF_{visc} and δF_p

$$\delta F = \delta F_{visc} + \delta F_p = \delta z(\int_L \tau_s \, dL) - \delta z s \nabla p_{elA}$$

where L is a contour formed with the crossing of the particle surface by the flatness, parallel to the base of cylinder, and s is the base area.

According to the second Newtonian law, force δF must be equal to the inertia force induced by the acceleration in the ultrasound wave. This inertia force is negligible when the pressure gradient in the ultrasound wave varies slowly with sound, which leads to the conclusion that at low frequencies the total force $\delta F = 0$. Thus, under this condition

$$\frac{1}{s}\int_L \tau_s \, dL = \nabla p_{elA} \tag{7A}$$

and, in accordance with eqs 6A and 7A, the macroscopic density of the streaming current that crosses the cylinder equals

$$\langle i \rangle = \frac{1}{s}\int_L I_s \, dL = \frac{\epsilon_m \zeta}{\eta} \nabla p_{elA}$$

Substituting ∇p_{elA} from eq 3A and taking into account eq 2A, we obtain the following relationship between the streaming current density inside the aggregate and the pressure gradient in the ultrasound wave:

$$\langle i \rangle = \frac{\epsilon_m \zeta}{\eta} q_{pA} \frac{\rho_p - \rho_m}{\rho_m} \nabla p$$

The contribution of the all aggregates to CVI in the dilute dispersion comes up as the streaming current in the aggregates multiplied by their volume fraction:

$$CVI_A = \frac{\epsilon_m \zeta}{\eta} q_{pA} q_A \frac{\rho_p - \rho_m}{\rho_m} \nabla p \tag{8A}$$

The product of volume fractions $q_{pA} q_A$ is just equal to the volume fraction of the dispersed phase in the aggregated dispersion:

$$q_{pA} q_A = q \tag{9A}$$

Therefore, this direct calculation of CVI in the aggregated dilute dispersion of particles with a thin DL and a small Dukhin number leads to the same result as eq 18 independently of the shape of particles and aggregates. The last one had been derived using the Onsager relationship. This means that our direct derivations basically confirmed the validity of the Onsager principle for electroacoustics in the aggregated system. The key point is the realization that the electric streaming current is proportional to the normal derivative of the tangential flow velocity but not to the liquid flow rate through the aggregate, which decreases for dense aggregates.

LA062612O